

Dislocation-enhanced piezoelectric catalysis of KNbO₃ crystal for water splitting

Hanyu Gong¹ | Jiawen Zhang² | Yan Zhao¹ | Shan Xiang¹ | Xiang Zhou¹ |
Oliver Preuß^{3,4} | Wenjun Lu² | Yan Zhang¹  | Xufei Fang⁴ 

¹State Key Laboratory of Powder Metallurgy, Central South University, Changsha, China

²Department of Mechanical and Energy Engineering, Southern University of Science and Technology, Shenzhen, China

³Department of Materials and Earth Sciences, Technical University of Darmstadt, Darmstadt, Germany

⁴Institute for Applied Materials, Karlsruhe Institute of Technology, Karlsruhe, Germany

Correspondence

Wenjun Lu, Department of Mechanical and Energy Engineering, Southern University of Science and Technology, Shenzhen 518055, China.

Email: luwj@sustech.edu.cn

Yan Zhang, State Key Laboratory of Powder Metallurgy, Central South University, Changsha, 410083, China.
Email: yanzhangcsu@csu.edu.cn

Xufei Fang, Institute for Applied Materials, Karlsruhe Institute of Technology, 76131 Karlsruhe, Germany.
Email: xufei.fang@kit.edu

Funding information

European Research Council, Grant/Award Number: 101076167; YIN Grant; Shenzhen Science and Technology Program, Grant/Award Number: JCYJ20230807093416034; Open Fund of the Microscopy Science and Technology-Songshan Lake Science City, Grant/Award Number: 202401204; National Natural Science Foundation of China, Grant/Award Number: 52371110; Guangdong Basic and Applied Basic Research Foundation, Grant/Award Number: 2023A1515011510

Abstract

Dislocations in oxides with ionic/covalent bonding hold potential for harnessing versatile functionalities. Here, high-density dislocations in a large plastic zone in potassium niobate (KNbO₃) crystals are mechanically introduced by room-temperature cyclic scratching to enhance piezocatalytic hydrogen production. Unlike conventional energy-intensive, time-consuming deformation at high temperature, this approach merits efficient dislocation engineering. These dislocations induce local strain and modify the electronic environment, thereby improving surface reactivity and charge separation, which are critical for piezocatalysis. This proof-of-concept offers a practical and sustainable alternative for functionalizing piezoelectric ceramics. Our findings demonstrate that surface-engineered dislocations can effectively improve the piezocatalysis, paving the way for efficient and scalable piezocatalytic applications.

KEY WORDS

dislocations, KNbO₃, piezocatalysis, room-temperature deformation, water splitting

Hanyu Gong and Jiawen Zhang contributed equally to this work and should be listed as co-first authors.

This is an open access article under the terms of the [Creative Commons Attribution](#) License, which permits use, distribution and reproduction in any medium, provided the original work is properly cited.

© 2025 The Author(s). *Journal of the American Ceramic Society* published by Wiley Periodicals LLC on behalf of American Ceramic Society.

1 | INTRODUCTION

Dislocations in ceramics have been recently discovered as a renewed tool for tuning the mechanical properties, such as plasticity,¹ strength,² and fracture resistance.³ However, their role in functional properties, especially in catalysis, has fallen short in exploration. Dislocations, atomic line distortion in crystalline solids, can introduce a local high-strain field⁴ and induce polar nanoregions, leading to a diverse ferroelectric domain structure.^{5,6} These features have the potential to influence catalytic performance by improving surface reactivity and facilitating charge separation.^{7,8} These effects are especially valuable in catalytic reactions, where surface-active sites are crucial for the adsorption and transformation of reactants.

Piezocatalysis,⁹ which utilizes the piezoelectric effect to drive catalytic reactions under mechanical stress, offers several advantages over traditional methods such as physical hydrogen evolution, photocatalysis, thermo-catalysis, and electrocatalysis. Compared with physical hydrogen evolution,¹⁰ the piezocatalytic process generates additional hydrogen, which is not a simple desorption-adsorption process but rather involves complex chemical transformations. Contrasting photocatalysis,^{11,12} which is limited by light availability and wavelength constraints, piezocatalysis can operate efficiently in the absence of light and is not restricted to a specific wavelength. Thermo-catalysis¹³ requires high temperatures and substantial energy input. Piezocatalysis works at room temperature, significantly reducing energy consumption. Furthermore, it does not rely on external electrical sources as electrocatalysis does, simplifying the system and reducing overall energy demand.¹⁴ These factors make piezocatalysis an attractive and energy-efficient alternative, particularly in applications like water splitting and hydrogen production.¹⁵ Our previous research¹⁶ on barium titanate (BaTiO_3) single crystals has shown that introducing dislocations can enhance piezocatalytic hydrogen production. However, this typical method for introducing dislocations into BaTiO_3 involves high-temperature mechanical imprinting,⁵ which is energy-intensive and results in dislocations being introduced deep within the crystal structure. Most of these internal dislocations are unlikely to effectively participate in surface catalytic reactions, which are essential for piezocatalysis. Unlike BaTiO_3 , which requires high-temperature processing for dislocation introduction, KNbO_3 is capable of room-temperature bulk deformation,¹⁷ allowing for the controlled introduction of dislocations at the material surface without the risk of fracture.² Furthermore, the high-temperature imprinting process requires expensive bulk crystals, which may also form cracks during compression and cooling, reducing the structural integrity and stability of cata-

lysts. Although strategies such as doping¹⁸ and oxygen-vacancy modification¹⁹ have been successfully employed to enhance the piezocatalytic water splitting performance of KNbO_3 , the piezocatalytic behavior of KNbO_3 single crystals containing dislocations has not yet been systematically explored, and their significant potential for hydrogen evolution remains to be further unveiled.

In this study, we explore an approach for enhancing the piezocatalytic performance of potassium niobate (KNbO_3) single crystals by introducing dislocations via mechanical scratching at room temperature. This method offers an energy-efficient alternative to traditional techniques and enhances the material's surface reactivity, leading to improved piezocatalytic hydrogen production. The findings demonstrate that surface-localized dislocations in KNbO_3 effectively improve its catalytic activity, offering a promising approach for piezocatalysis without the need for the costly high-temperature treatment. This work aims to provide a more sustainable and efficient strategy for functionalizing piezoelectric ceramics in catalytic applications.

2 | MATERIALS AND EXPERIMENTS

Undoped KNbO_3 (KNO) single crystals (FEE GmbH), grown by the top-seeded solution method, were used for this study. At room temperature, KNO has an orthorhombic crystal structure. As the temperature increases, it undergoes two phase transitions from orthorhombic to tetragonal at 225°C, then to cubic at 435°C.²⁰ The crystallographic directions used later are the pseudo-cubic directions^{20,21} for consistency of room-temperature slip system definition as in other perovskite oxides such as SrTiO_3 and KTaO_3 , both of which have a cubic structure at room temperature. The samples were cut into the dimensions of about 5 mm × 5 mm × 1 mm with the large surface being (001). The (001) surfaces were sequentially ground with wet grinding papers (P800, P1200, P2500, and P4000, QATM). Then the samples were further polished (Phoenix 4000, Buehler) with diamond polishing paste (particle sizes being 6, 3, 1, and 1/4 μm) for 30 min each. A final step of vibrational polishing was adopted using OPS polishing solution containing ~50 nm colloidal silica particles for 20 h. This detailed procedure has proven to be effective in removing grinding/polishing-induced unintended near-surface damage.

To intentionally engineer high-density dislocations, the cyclic Brinell indenter scratching method²² was adopted at room temperature using a universal hardness testing machine (Finotest, Karl-Frank GmbH), which is mounted with a spherical indenter made of hardened steel, with a diameter of 2.5 mm. The Brinell indenter was brought

into contact with the sample (001) surface with a load of 0.8 kg to slide along the $<110>$ direction at a velocity of 0.5 mm s^{-1} , controlled by a single-axis piezo stage (PI Instruments). To increase the dislocation density inside the scratch tracks, 10 passes ($10\times$) were used for each scratch track.²³ Silicone oil was used as a lubricant during the scratch tests. The region affected by the plastic deformation (single scratch track) has a width of $\sim 150 \mu\text{m}$ and a depth of tens of micrometers. To enlarge the plastic zone, multiple parallel scratch tracks were overlapped on the (001) surface to create a region of about $3 \text{ mm} \times 3 \text{ mm}$ dislocation zone (see Figure S1).

To characterize the generated dislocations via Brinell indenter scratching, we used electron channeling contrast imaging (ECCI) within an SEM (scanning electron microscopy, Tescan MIRA3-XM) equipped with a four-quadrant solid-state BSE detector (DEBEN). The acceleration voltage was 15 kV with a working distance of 8 mm. A carbon layer of approximately 10 nm thickness was sputtered on top of the sample to reduce the surface charging effect. As ECCI is a surface imaging technique, for in-depth and cross-sectional visualization of the dislocations, TEM (transmission electron microscope) specimens were prepared inside the plastic zone, along the $<100>$ orientation, using a dual-beam focused ion beam (FIB, Helios Nanolab 600i, FEI). Annular dark field scanning TEM (ADF-STEM) imaging was performed on a TEM instrument (FEI Talos F200X G2, Thermo Fisher Scientific) at an operating voltage of 200 kV. A probe semiconvergence angle of 10.5 mrad and inner and outer semicollection angles of 23–55 mrad were used in the ADF-STEM imaging. Atomic-scale TEM analysis was performed on a double aberration-corrected TEM (TitanThemis G2, FEI) operating at 300 kV. A probe semiconvergence angle of 17 mrad and an inner and outer semicollection angle of 38–200 mrad were used for high-angle annular dark field STEM (HAADF-STEM) imaging.

Piezoelectric hydrogen production was conducted in a closed glass vessel with a volume of 713 mL. A KNbO₃ single crystal was placed into a glass vessel containing 35 mL of pure water, without any sacrificial agents. After absorption in water for 30 min, nitrogen (N₂) was passed through the solution with a gas flow rate of 8 L/h for 15 min to obtain an inert atmosphere. Subsequently, the piezocatalysis was conducted in an ultrasonic bath for 30 min with an ultrasonic frequency of 45 kHz and a power of 600 W. Then the instantaneous yield of H₂ (Y_H) at intervals of 30 min was measured by the gas chromatograph (UATEC-6600, Fanwei (Shanghai) Analytical Instruments Co., LTD) equipped with thermal conductivity detector (EHP15887, Valco Instruments Co. Inc.). The detection limit of the thermal conductivity detector is 10^{-3} ppm, and the piezocatalytic H₂ production rate was calculated by

Equation (1)²⁴:

$$v = Y_H V / V_m t, \quad (1)$$

where V is the total gas volume of the closed glass vessel, and V_m is the ideal molar volume of gas, which is 22.4 L/mol , and t is the reaction time.

3 | RESULTS AND ANALYSES

ADF-STEM analysis reveals the dislocation distribution and dislocation structure of the (001) KNbO₃ single crystal with $10\times$ scratching. As displayed in Figure 1A, the dislocation density reaches $\sim 10^{14} \text{ m}^{-2}$ after $10\times$ scratching, and the dislocations are mainly composed of long 45° segments (marked by the blue arrows in Figure 1B) and irregular segments (marked by the green arrows in Figure 1B). In several oxide ceramics with room-temperature bulk plasticity, mechanical scratching drives dislocations to depths beyond $100 \mu\text{m}$,^{25,26} ensuring their persistence against ultrasonic dissolution and sustaining catalytic performance. Two-beam analysis along different diffraction conditions was then employed to confirm the Burgers vector of the dislocation lines generated by cyclic scratching. As demonstrated in Figure 1D, the 45° segments were invisible along the diffraction vector $\mathbf{g} = 1\bar{1}0$, while visible along the other diffraction conditions in Figure 1. Hence, the dislocation Burgers vector \mathbf{b} yields [110]. The dislocation line vector \mathbf{t} was determined to [110] by the dislocation analysis along the $<001>$ zone axis. Since the dislocation Burgers vector is parallel to the line vector, these 45° dislocation segments are confirmed as screw-type dislocations, and belong to the $<110> \{110\}$ slip system.²⁷ The irregular dislocation segments were invisible along the diffraction vector $\mathbf{g} = 100$, which yields an uncertain Burgers vector of [001], [101], or [101].

We then used the HAADF-STEM imaging, coupled with fast Fourier transform (FFT) and inverse FFT (IFFT), to investigate the core structures of the head or tail of the 45° dislocation segments, as illustrated in Figure 2. Here again, we use a pseudo-cubic (pc) cell to index diffraction patterns in the orthorhombic (ortho) cell for clarity, namely, $[110]_{\text{ortho}} = [100]_{\text{pc}}$, $[110]_{\text{ortho}} = [010]_{\text{pc}}$, and $[001]_{\text{ortho}} = [001]_{\text{pc}}$. At the head of the 45° dislocation dipole marked by the blue box in Figure 2A, we identified two edge-type dislocations with opposite Burgers vectors of $1/2a[110]_{\text{pc}}$ and $1/2a[\bar{1}\bar{1}0]_{\text{pc}}$, respectively (Figure 2B). The IFFT pattern in Figure 2C reveals that the dislocation dipole was separated by a distance of multiple unit cells ($\sim 7 \text{ nm}$). At the tail of the single 45° dislocation segment marked by the green box in Figure 2A, we identified two glide dissociated edge dislocations with the same Burgers

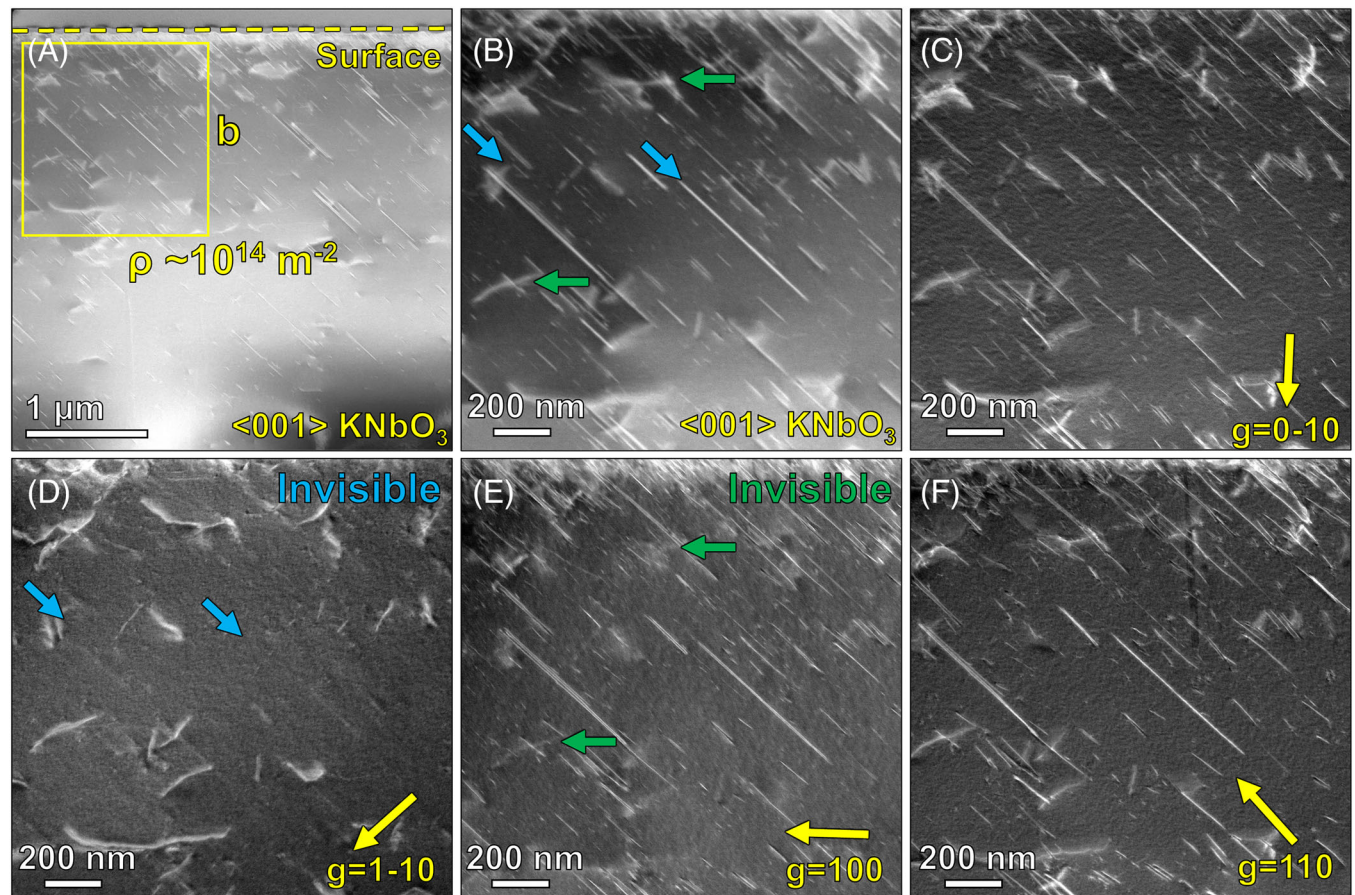


FIGURE 1 ADF-STEM images of dislocations in (001) KNbO_3 with 10 \times scratching under different diffraction conditions. (A) Dislocation distribution of the 10 \times scratched (001) KNbO_3 with a density of $\sim 10^{14} \text{ m}^{-2}$; change of the dislocation contrast along (B) $<001>$ zone axis, (C) $\mathbf{g} = 0\bar{1}0$, (D) $\mathbf{g} = 1\bar{1}0$, (E) $\mathbf{g} = 100$, (F) $\mathbf{g} = 110$.

vector of $1/2\mathbf{a}[\bar{1}\bar{1}0]_{pc}$. The corresponding IFFT pattern in Figure 2E reveals that the distance between the partial dislocations is ~ 5 nm. The geometric phase analysis (GPA) map in Figure 2F generated by the FFT pattern insert, demonstrates the strain field distribution around the two edge dislocations. Two selected \mathbf{g} vectors, $\mathbf{g} = 100$ and $\mathbf{g} = 0\bar{2}0$, marked with blue circles in the FFT pattern, were used to compute the strain field in the x direction (ϵ_{xx}). The resulting strain map in Figure 2F revealed the areas of tensile strain (red) and compressive strain (blue) around the two edge dislocations, which exhibit an extremely high gradient.

Figure 3A displays the H_2 yield using reference and dislocation-rich KNO crystals as the piezocatalysts. For a blank control group, the average H_2 yield is 0.84 ppm, demonstrating the negligible H_2 production performance of the reactor. The average H_2 yield of the dislocation-rich sample is 77.04 ppm, which is 2.46 times higher than that of the reference sample. As shown in Figure 3B, after deducting H_2 mass produced by the reactor, the average H_2

production rate of the reference and deformed sample is 1.84 and 4.61 $\mu\text{mol}/\text{h}$, respectively. Figure 3C presents the comparison of the H_2 production rate between KNO single crystals with/without dislocations and other reported piezocatalysts. Due to a well-aligned domain structure,²⁸ deformed KNO exhibits a higher H_2 production rate than other polycrystalline bulk ceramics. Compared with the BaTiO_3 single crystal, a superior H_2 production performance of the deformed sample can be attributed to its stability in polarization at high temperature. Since the Curie temperature T_c of BaTiO_3 ($\sim 130^\circ\text{C}$)¹⁶ is lower than that of KNO ($>400^\circ\text{C}$),²⁹ higher temperatures caused by collapsed cavitation bubbles during the ultrasonic process may lead to a depolarization in BaTiO_3 and slower H_2 evolution. Furthermore, dislocation engineering is expected to further elevate the H_2 production rate, rendering it comparable to certain powder-based catalysts, such as nanowires with a high length-diameter ratio and strong piezoelectric potential,³⁰ and in this work, it already achieves about 17% of that obtained with potassium niobate powders.¹⁸

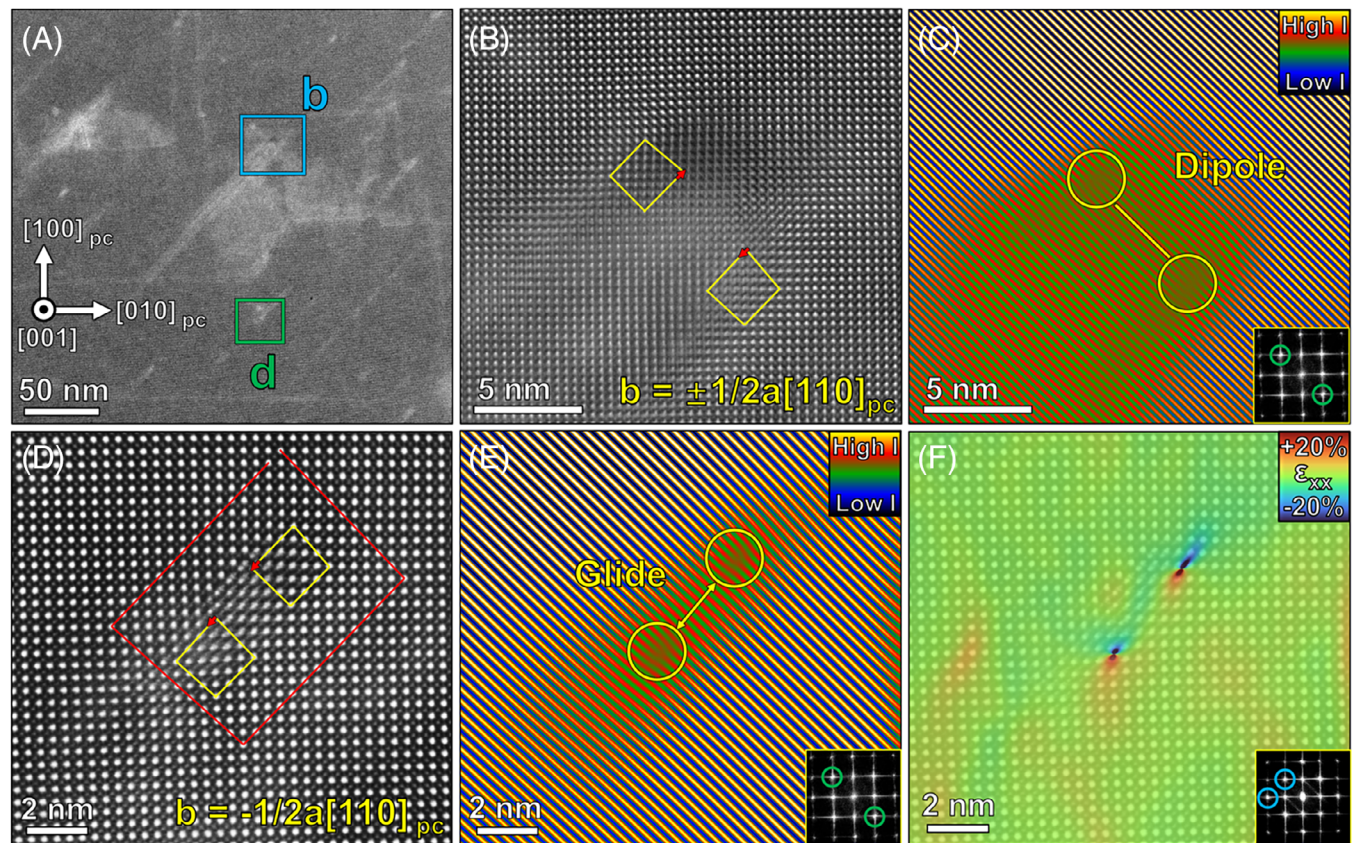


FIGURE 2 Dislocations in the 10 \times scratched (001) KNbO₃: (A) Low magnification of the 45°-inclined dislocation lines. (B) Dislocation core structure of the head of the 45° dislocation dipole marked in the blue box in (A), which includes two edge dislocations with opposite Burgers vectors. (C) An IFFT pattern in (B) shows the atom planes. (D) Dislocation core structure of the tail of the 45° dislocation line, containing two glide dissociated edge dislocations with the same Burgers vector. (E) An IFFT pattern in (D) shows the atom planes. (F) A GPA result reveals the strain distribution around the dislocation cores in (D).

4 | DISCUSSION

We discuss in Figure 4A, the possible mechanism based on screening the charge effect in piezocatalysis.³⁷ Initially, KNO remains electrically neutral as the bound charges induced by spontaneous polarization P_1 are compensated by oppositely charged external screening charges located at the two polar surfaces. When subjected to compressive stress, such as that induced by cavitation bubbles during ultrasonic treatment, the original charge equilibrium is disturbed. This leads to a lower polarization P_2 and the subsequent release of excess surface charges. These released charges will participate in redox reactions with surrounding species, including water molecules, dissolved oxygen, hydroxide ions (OH⁻), and protons (H⁺), until a new electrostatic equilibrium is established.^{24,37} Upon removal of the external stress, the polarization is restored from P_2 to P_1 , increasing polarization-associated bound charges, followed by absorbing free charges from the ambient environment and triggering new redox reactions. Subsequently, the KNO crystal returns to the initial

state. It should be noted that the primary difference between the deformed and reference samples lies in polarization and the piezoelectric coefficient d_{33}^* . Although mechanical scratching slightly modifies the surface morphology, our previous work^{25,26} demonstrated that the resulting change in surface area is minimal and can be neglected. Previous study³⁸ has also confirmed local polarization and d_{33}^* enhancement near a single dislocation. Furthermore, the higher spontaneous polarization P_s has been obtained in (K, Na)NbO₃ single crystals with internal stress, consequently contributing to a larger local piezoelectric coefficient d_{33}^* (Figure S3).^{5,39} Thus, compared with the reference sample (Figure 4B), the deformed sample (Figure 4C) exhibits a higher local strain ϵ (see GPA results in Figure 2F). The high strain and stress fields in the vicinity of dislocations,⁴⁰ as illustrated by the red region in Figure 4C, require additional bound polarization charges to compensate for the enhanced built-in electric field induced by the dislocations. This effect is particularly pronounced in the dislocation core region. Furthermore, previous work¹⁶ has

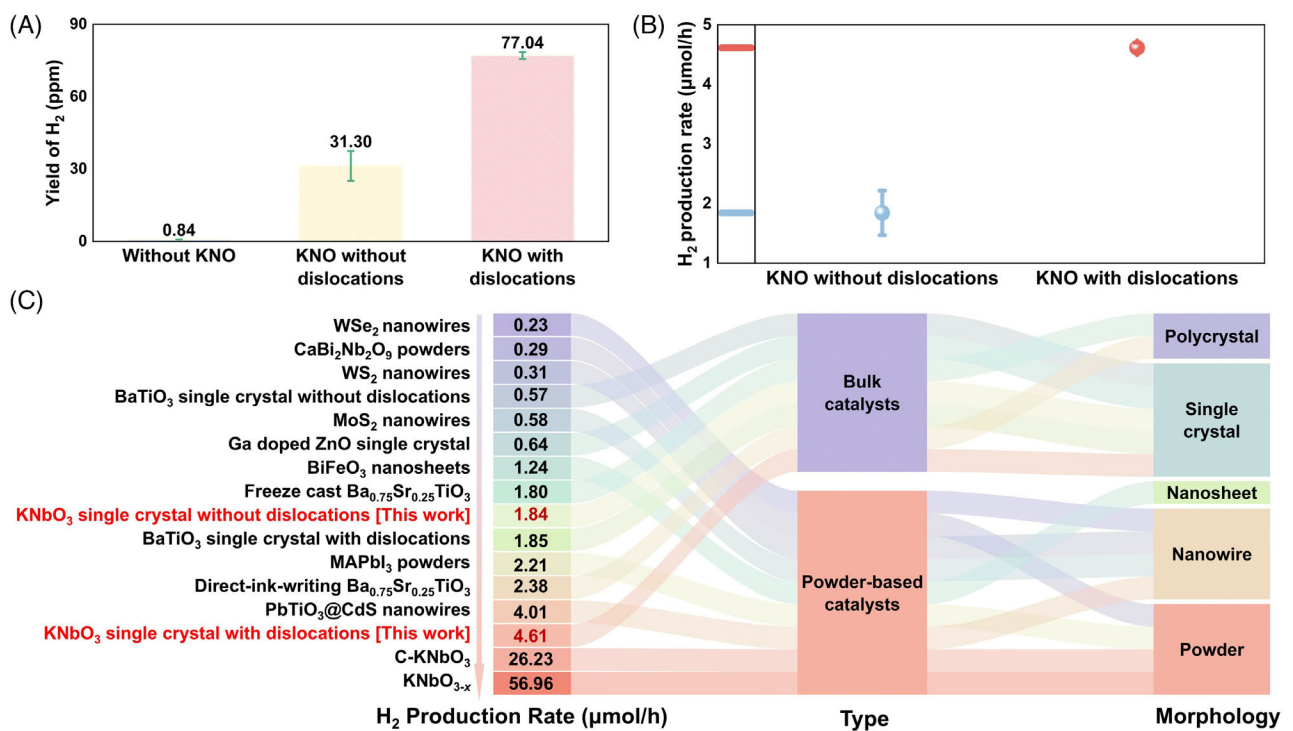


FIGURE 3 Performance of piezocatalytic hydrogen production. (A) Yield of hydrogen, (B) hydrogen production rate in KNbO₃ single crystal, (C) a comprehensive comparison of piezocatalysts in hydrogen production rate. ^{16,18,19,24,31–36}

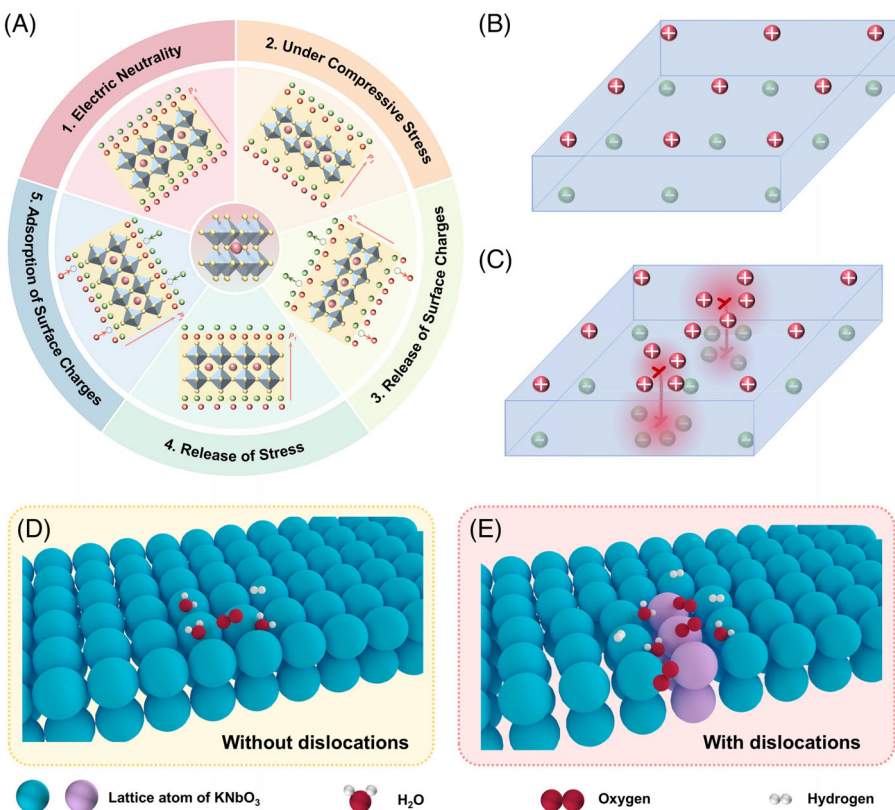


FIGURE 4 Mechanism of piezocatalytic hydrogen production. (A) Schematic of the screening charge effect. Schematic illustrations of KNbO₃ single crystals (B, D) without and (C, E) with dislocations, showing differences in surface charge distribution and water splitting process.

shown that dislocations can enhance electrical conductivity, resulting in faster release and accumulation of surface charges. As shown in the schematic diagram of Figure 4B,C, KNO with dislocations can produce more hydrogen and oxygen, which benefits from its higher local polarization.

5 | CONCLUSION

In summary, dislocations were successfully introduced into the near-surface region of bulk potassium niobate (KNbO_3) single crystals through room-temperature cyclic scratching, enabling a notable enhancement by more than two times in piezocatalytic hydrogen production rate. Compared with conventional high-temperature imprinting, this method is more energy-efficient and avoids the risk of crack formation or structural degradation. The improved catalytic performance is proposed to be primarily attributed to the elevated polarization level induced by strain fields surrounding the dislocations, which promotes more efficient charge separation and accelerates surface redox reactions. These findings demonstrate that mechanical deformation-based dislocation engineering at room temperature provides a feasible and potentially scalable approach to enhance the catalytic functionality of piezoelectric materials without additional chemical dopants or compromising structural integrity.

ACKNOWLEDGMENTS

X. Fang thanks the funding by the European Research Council (ERC Starting Grant, Project MECERDIS, no. 101076167) and the YIN (Young Investigator Network) grant at Karlsruhe Institute of Technology (KIT). W. Lu acknowledges the support by Shenzhen Science and Technology Program (grant no. JCYJ20230807093416034), the Open Fund of the Microscopy Science and Technology-Songshan Lake Science City (grant no. 202401204), National Natural Science Foundation of China (grant no. 52371110), and Guangdong Basic and Applied Basic Research Foundation (grant no. 2023A1515011510). The authors also acknowledge the use of the facilities at the Southern University of Science and Technology Core Research Facility and the State Key Laboratory of Powder Metallurgy of Central South University. The PFM images by Dr. F. Zhuo, ECCI images by Dr. E. Bruder, and helpful discussion and input by Prof. J. Rödel at TU Darmstadt are acknowledged.

Open access funding enabled and organized by Projekt DEAL.

CONFLICT OF INTEREST STATEMENT

The authors declare no conflict of interest.

DATA AVAILABILITY STATEMENT

The data used for this publication have been included in the manuscript or supplementary materials.

ORCID

Yan Zhang  <https://orcid.org/0000-0002-0132-3325>

Xufei Fang  <https://orcid.org/0000-0002-3887-0111>

REFERENCES

1. Oshima Y, Nakamura K, Matsunaga A. Extraordinary plasticity of an inorganic semiconductor in darkness. *Science*. 2018;360:772–74. <https://doi.org/10.1126/science.aar6035>
2. Zhang J, Fang W, Lu X. Impact of dislocation densities on the microscale strength of single-crystal strontium titanate. *Acta Mater*. 2025;291:121004. <https://doi.org/10.1016/j.actamat.2025.121004>
3. Fang X, Lu W, Zhang J, Minnert C, Hou J, Bruns S, et al. Harvesting room-temperature plasticity in ceramics by mechanically seeded dislocations. *Mater Today*. 2025;82:81–91. <https://doi.org/10.1016/j.mattod.2024.11.014>
4. Li T, Deng S, Liu J, Chen H. Insights into strain engineering: from ferroelectrics to related functional materials and beyond. *Chem Rev*. 2024;124:7045–105. <https://doi.org/10.1021/acs.chemrev.3c00767>
5. Höfling M, Zhou X, Riemer LM, Bruder E, Liu B, Zhou L, et al. Control of polarization in bulk ferroelectrics by mechanical dislocation imprint. *Science*. 2021;372:961–64. <https://doi.org/10.1126/science.abe3810>
6. Park S, Choi H, Hwang G-T, Peddigari M, Ahn C-W, Hahn B-D, et al. Molten-salt processed potassium sodium niobate single-crystal microcuboids with dislocation-induced nanodomain structures and relaxor ferroelectric behavior. *ACS Nano*. 2022;16:15328–38. <https://doi.org/10.1021/acsnano.2c06919>
7. Wang J, Li K, Guo L, Pan B, Jin T, Li Z, et al. Lattice strain and surface activity of dislocation-distorted agpd nanoalloys under preoxidation and catalysis condition. *Small Struct*. 2023;4:2300169. <https://doi.org/10.1002/sstr.202300169>
8. Muhammad QK, Valderrama M, Yue M, Opitz AK, Taibl S, Siebenhofer M, et al. Dislocation-tuned electrical conductivity in solid electrolytes (9YSZ): a micro-mechanical approach. *J Am Ceram Soc*. 2023;106:6705–16. <https://doi.org/10.1111/jace.19291>
9. Tu S, Guo Y, Zhang Y, Hu C, Zhang T, Ma T, et al. Piezocatalysis and piezo-photocatalysis: catalysts classification and modification strategy, reaction mechanism, and practical application. *Adv Funct Mater*. 2020;30:2005158. <https://doi.org/10.1002/adfm.202005158>
10. Tao G, Zhang H, Li A, Xue X, Zhang Y, Zhang Y, et al. Effect of alloy particle size and device internal structure on the de-/hydriding properties of Ti-Zr-Cr-Mn based hydrogen storage alloys. *Int J Hydrogen Energy*. 2025;173:151029. <https://doi.org/10.1016/j.ijhydene.2025.151029>
11. Tong H, Ouyang S, Bi Y, Umezawa N, Oshikiri J, Ye M. Nano-photocatalytic materials: possibilities and challenges. *Adv Mater*. 2012;24:229–51. <https://doi.org/10.1002/adma.201102752>
12. Kalia R, Yadav P, Verma A, Yadav BS, Naidu J. Natural sunlight induced photocatalytic hydrogen evolution by $\text{SrTaO}_2\text{N}/\text{CdS}$

nanocomposites. *J Alloys Compd.* 2025;1015:178790. <https://doi.org/10.1016/j.jallcom.2025.178790>

- 13. Peng M, Ge Y, Gao R, Yang J, Li A, Xie Z, et al. Thermal catalytic reforming for hydrogen production with zero CO₂ emission. *Science*. 2025;387:769–75. <https://doi.org/10.1126/science.adt0682>
- 14. Li Y, Wang H, Priest C, Li S, Xu G, Wu P. Advanced electrocatalysis for energy and environmental sustainability via water and nitrogen reactions. *Adv Mater.* 2021;33:e2000381. <https://doi.org/10.1002/adma.202000381>
- 15. Li S, Zhang X, Yang F, Zhang J, Shi F, Rosei W. Mechanically driven water splitting over piezoelectric nanomaterials. *Chem Catal.* 2024;4:100901.
- 16. Zhang Y, Feng K, Song M, Xiang S, Zhao Y, Gong H, et al. Dislocation-engineered piezocatalytic water splitting in single-crystal BaTiO₃. *Energy Environ Sci.* 2025;18:602–12. <https://doi.org/10.1039/D4EE03789H>
- 17. Frisch A, Okafor C, Preuß O, Zhang J, Matsunaga K, Nakamura A, et al. Room-temperature dislocation plasticity in ceramics: methods, materials, and mechanisms. *J Am Ceram Soc.* 2025;108:e20575. <https://doi.org/10.1111/jace.20575>
- 18. He J, Gao F, Wang H, Liu F, Lin J, Wang B, et al. C-doped KNbO₃ single crystals for enhanced piezocatalytic intermediate water splitting. *Environ Sci: Nano.* 2022;9:1952–60.
- 19. Tan H-Y, Zhan L, Yan C-F, Abeykoon LK, De Silva J, Bandara NL. Enhancement of the conversion of mechanical energy into chemical energy by using piezoelectric KNbO_{3-x} with oxygen vacancies as a novel piezocatalyst. *Nano Express.* 2020;1:030036. <https://doi.org/10.1088/2632-959X/abd290>
- 20. Hirel P, Mark AF, Castillo-Rodriguez M, Sigle W, Mrovec C, Elsässer M. Theoretical and experimental study of the core structure and mobility of dislocations and their influence on the ferroelectric polarization in perovskite KNbO₃. *Phys Rev B.* 2015;92:214101. <https://doi.org/10.1103/PhysRevB.92.214101>
- 21. Preuß O, Bruder E, Lu W, Zhuo F, Minnert C, Zhang J, et al. Dislocation toughening in single-crystal KNbO₃. *J Am Ceram Soc.* 2023;106:4371–81.
- 22. Fang X, Preuß O, Breckner P, Zhang W, Lu J. Engineering dislocation-rich plastic zones in ceramics via room-temperature scratching. *J Am Ceram Soc.* 2023;106:4540–45. <https://doi.org/10.1111/jace.19140>
- 23. Drechsler F, Hincinschi C, Preuß O, Fang J, Kortus X. Dislocation-induced local symmetry reduction in single-crystal KNbO₃ observed by Raman spectroscopy. *J Am Ceram Soc.* 2025;108:e20221. <https://doi.org/10.1111/jace.20221>
- 24. Gong H, Zhang Y, Ye J, Zhou X, Zhou X, Zhao Y, et al. Retrievable hierarchically porous ferroelectric ceramics for “greening” the piezo-catalysis process. *Adv Funct Mater.* 2024;34:2311091. <https://doi.org/10.1002/adfm.202311091>
- 25. Preuß O, Bruder E, Zhang J, Lu W, Rödel J, Fang X. Damage-tolerant oxides by imprint of an ultra-high dislocation density. *J Eur Ceram Soc.* 2025;45:116969.
- 26. Fang X, Preuß O, Breckner P, Zhang W, Lu J. Engineering dislocation-rich plastic zones in ceramics via room-temperature scratching. *J Am Ceram Soc.* 2023;106:4540–45. <https://doi.org/10.1111/jace.19140>
- 27. Mark AF, Castillo-Rodriguez W, Sigle M. Unexpected plasticity of potassium niobate during compression between room temperature and 900°C. *J Eur Ceram Soc.* 2016;36:2781–93. <https://doi.org/10.1016/j.jeurceramsoc.2016.04.032>
- 28. Wada S, Muraoka K, Kakemoto H, Tsurumi H, Kumagai T. Enhanced piezoelectric properties of potassium niobate single crystals with fine engineered domain configurations. *Materials Science and Engineering: B.* 2005;120:186–89. <https://doi.org/10.1016/j.mseb.2005.02.033>
- 29. Hewat AW. Cubic-tetragonal-orthorhombic-rhombohedral ferroelectric transitions in perovskite potassium niobate: neutron powder profile refinement of the structures. *J Phys C: Solid State Phys.* 1973;6:2559–72. <https://doi.org/10.1088/0022-3719/6/16/010>
- 30. Liu Q, Zhai D, Xiao Z, Tang C, Sun Q, Bowen CR, et al. Piezo-photocatalytic coupling effect of BaTiO₃@TiO₂ nanowires for highly concentrated dye degradation. *Nano Energy.* 2022;92:106702. <https://doi.org/10.1016/j.nanoen.2021.106702>
- 31. Li S, Zhao Z, Yu D, Zhao J-Z, Su Y, Liu Y, et al. Few-layer transition metal dichalcogenides (MoS₂, WS₂, and WSe₂) for water splitting and degradation of organic pollutants: understanding the piezocatalytic effect. *Nano Energy.* 2019;66:104083. <https://doi.org/10.1016/j.nanoen.2019.104083>
- 32. Liu Q, Zhan F, Luo H, Luo X, Yi Q, Sun Q, et al. Na-Sm bimetallic regulation and band structure engineering in CaBi₂Nb₂O₉ to enhance piezo-photo-catalytic performance. *Adv Funct Mater.* 2023;33:2303736. <https://doi.org/10.1002/adfm.202303736>
- 33. Wang B, Zhang Q, He J, Huang F, Li M, Wang C. Co-catalyst-free large ZnO single crystal for high-efficiency piezocatalytic hydrogen evolution from pure water. *J Energy Chem.* 2022;65:304–11. <https://doi.org/10.1016/j.jechem.2021.06.004>
- 34. You H, Wu Z, Zhang L, Ying Y, Liu Y, Fei L, et al. Harvesting the vibration energy of BiFeO₃ nanosheets for hydrogen evolution. *Angew Chem Int Ed.* 2019;58:11779–84. <https://doi.org/10.1002/anie.201906181>
- 35. Wang M, Zuo Y, Wang J, Wang Y, Shen X, Qiu B, et al. Remarkably enhanced hydrogen generation of organolead halide perovskites via piezocatalysis and photocatalysis. *Adv Energy Mater.* 2019;9:1901801. <https://doi.org/10.1002/aenm.201901801>
- 36. Huang X, Lei R, Yuan J, Gao F, Jiang C, Feng W, et al. Insight into the piezo-photo coupling effect of PbTiO₃/CdS composites for piezo-photocatalytic hydrogen production. *Appl Catal, B.* 2021;282:119586. <https://doi.org/10.1016/j.apcatb.2020.119586>
- 37. Wang K, Han C, Li J, Qiu J, Sunarso S, Liu J. The mechanism of piezocatalysis: energy band theory or screening charge effect? *Angew Chem Int Ed.* 2022;61:e202110429. <https://doi.org/10.1002/anie.202110429>
- 38. Li N, Zhu R, Cheng X, Liu H-J, Zhang Z, Huang Y-L, et al. Dislocation-induced large local polarization inhomogeneity of ferroelectric materials. *Scr Mater.* 2021;194:113624. <https://doi.org/10.1016/j.scriptamat.2020.11.009>
- 39. Zhao G, Liu L, Tian G, Yin F, Yan Q, Wang J, et al. Large piezoelectricity induced by internal stress in (K,Na)NbO₃ single crystals. *ACS Appl Mater Interfaces.* 2024;16:41194–201. <https://doi.org/10.1021/acsami.4c10010>

40. Hull D, Bacon DJ. Chapter 4 - Elastic properties of dislocations, in *Introduction to dislocations*. 5th ed. Oxford: Butterworth-Heinemann, 2011.

SUPPORTING INFORMATION

Additional supporting information can be found online in the Supporting Information section at the end of this article.

How to cite this article: Gong H, Zhang J, Zhao Y, Xiang S, Zhou X, Preuß O, et al.

Dislocation-enhanced piezoelectric catalysis of KNbO_3 crystal for water splitting. *J Am Ceram Soc.* 2026;109:e70414. <https://doi.org/10.1111/jace.70414>